DISC: A Novel Distributed On-Demand Clustering Protocol for Internet of Multimedia Things

Amrita Ghosal, Subir Halder and Mauro Conti, *IEEE Senior Member*
Department of Mathematics
University of Padua, Italy
{amrita.ghosal, subir.halder, conti}@math.unipd.it

***Abstract*—Internet of Multimedia Things (IoMT) are receiving significant attention due to a wide variety of applications, e.g., wildlife habitat monitoring, but they are often highly resource constrained. Compared to Internet of Things, preserving battery power of nodes, and maximizing the lifespan of IoMT are more critical and challenging as sensed data are mostly image/video instead of simple scalar. Recent studies have shown that clustering is an efficient solution to reduce energy consumption. In clusters, the role of each node changes to reduce energy consumption, thereby, prolonging lifespan. In this paper, we address the lifespan maximization problem in IoMT by designing a clustering protocol where clusters are formed dynamically. Specifically, we analyze and solve an optimization problem aiming to maximize the lifespan by reducing the energy consumption among cluster heads. Based on the analysis, we propose a novel DIStributed on-demand Clustering (DISC) protocol. Our cluster head election procedure is not periodic, but adaptive, based on the dynamism of the occurrence of events. This on-demand execution of DISC aims to significantly reduce computation and message overheads. We validate the performance of DISC through extensive experiments. Experimental results show that DISC is 25% more energy balanced and achieves 32% more lifespan as compared to two state-of-the-art solutions.**

***Index Terms*—Energy balance, Linear programming, Network lifespan, Clustering, Internet of Multimedia Things.**

I. Introduction

Due to the impetuous advancement of technologies in recent years, the integration of wireless cameras with Internet of Things (IoT) [1] has started to receive attention in various cyber-physical systems including environment monitoring, public safety, and wildlife tracking [2]. Such networks, referred to as Internet of Multimedia Things (IoMT) [2], deploy certain number of cameras in addition to other types of scalar sensors (e.g., temperature, light), and can gather and process multimedia data. One example is smart wildlife tracking system, where several video analyses, and computer vision algorithms, e.g., tracking, and behaviour analysis, are integrated into smart sensor nodes for large scale wildlife tracking. In many cases, multimedia nodes (henceforth, referred to as IoMT nodes or nodes) are battery powered with a limited capacity, and hardly last for few months or at the most for a year. Therefore, energy is the scarcest resource in IoMT due to the difficulty of replacing or efficiently recharging batteries in remote or hostile environments. In IoMT, unlike IoT, generally sensed data are mostly image/video instead of simple scalar, which require much more energy for transmitting, and gathering. Also, processing image/video data requires more complex and energy consuming techniques. Hence, in IoT, where energy consumption is dominated only by data transmission and reception, IoMT consumes extra energy on image/video data capturing, processing, and storage operations. These additional energy consumption has a significant effect on the battery power, and leads to premature decrease of network lifespan in IoMT.

Different studies [3], [4] have shown that clustering is an efficient solution to reduce energy consumption among nodes. Particularly, schemes based on clustering technique aim to organize the network topology in a way that the role of individual nodes changes to minimize energy consumption. The focus of this paper is thus on works specifically targeted to clustering techniques. In clustering paradigm, each cluster has a coordinator, referred to as Cluster Head (CH) and a number of Member Nodes (MNs). The MNs capture image/video data from the environment and transmit their data to the respective CHs. In general, data gathered by the CHs are often redundant and highly correlated in nature. Hence, to reduce the redundant data, the CHs aggregate the data, and send them to the sink, either directly or via a multi-hop path. Apart from data aggregation, the network may be reclustered periodically to select energy abundant nodes to function as CHs, thus, distributing the load uniformly on all the nodes. Since significant numbers of nodes are deployed in IoMT, so green networking plays a crucial role in IoMT to reduce energy consumption, lessen pollution and emissions. Besides energy saving capability, clustering reduces channel contention and packet collisions, resulting in better network throughput [4].

Based on the clustering properties, we classified the existing techniques into two categories, namely, uniform clustering and non-uniform clustering. In uniform clustering [5], the clusters with relatively equal sizes are formed, to keep the number of clusters as small as possible, evenly distribute them across the network, and typically, provide minimum overlapping among them. The major problem in uniform clustering is that the traffic load is not evenly distributed among all the nodes. Particularly, the nodes located nearer to the sink bear more traffic load than those farther away from the sink, eventually resulting in the energy hole problem [4]. On the contrary, in non-uniform clustering [6], based on the distance between the nodes and the sink, variable sizes of clusters are formed across the network to evenly distribute the traffic load among the nodes. Since the traffic load among the nodes are distributed

evenly, non-uniform clustering is more promising with respect to energy efficiency than uniform clustering.

In this work, we consider non-uniform clustering. Further, to reduce energy consumption of the data gathering process, we consider event driven based data gathering [7], and cluster formation is triggered by occurrence of event, i.e., on-demand based. In the on-demand based clustering, a node wakes up only when an event is detected or another node wants to communicate with it. While the application of the on-demand based clustering strategy is not limited to a specific example, to help the reader understand our solution, we assume the following scenario. Let us assume a IoMT deployed for monitoring a parking lot, where IoMT nodes are deployed in a large building, each IoMT node is equipped with a camera for taking images once an intruder is detected. In presence of obstacles, a IoMT node may capture a limited view of the intruder. IoMT nodes thus form clusters according to on-demand basis. Thereafter, the CH collects the captured images from IoMT nodes (or, MNs) to build the complete view of the region that is being monitored along with the intruder.

Many clustering techniques [5], [6], [8], [9] have been designed to balance energy consumption. Most of the proposed strategies consider time driven based clustering and ideal channel model. Furthermore, in existing clustering approaches, CHs are either pre-assigned [5], [8] or selected based on residual energy [9], [10]. The major problems of pre-assigned clustering approaches are that they are neither dynamic nor energy efficient, and have limited applications. In contrast, our proposed clustering strategy is dynamic, and CHs are selected based on the average energy usage and residual energy level. To the best of our knowledge, there exists no literature that considers optimization of cluster size by including realistic channel model to minimize and balance energy consumption among CHs, while devising clustering protocol for IoMT. The major contributions of this paper are as follows:

- First, we analyze the role of cluster radius in energy balancing and network lifespan maximization by considering the impacts of both inter-cluster and intra-cluster data traffic. Our analytical results show that choosing of appropriate cluster radius (i.e., decreasing trend towards the sink) has significant role in maximizing network lifespan.
- Based on the analysis, we derive the principle of optimal clustering structure and that, in turn, is used to compute the optimal cluster radius.
- Different from the existing protocols, we next propose a novel DIStributed on-demand Clustering (DISC) protocol, where CHs are selected dynamically based on the average energy usage and residual energy level. The invocation of DISC is based on the detection of an event of interest. This reduces the unnecessary system updates and hence computation and message overheads.
- Through extensive simulation, we show that DISC achieves higher energy efficiency and network lifespan than existing approaches [6], [9] under both indoor and outdoor environments. Moreover, non-uniform clustering in IoMT offers more efficiency in energy savings, and prolonged lifespan compared to traditional IoT network.

The rest of this paper is organized as follows. Section II discusses the related works. The system model considered for the present work is described in Section III. Section IV theoretically analyzes the network lifespan maximization problem and obtains the optimal clustering strategy. The proposed clustering strategy is described in Section V. Section VI presents experimental results under indoor and outdoor environmental conditions. Finally, concluding remarks are given in Section VII.

II. Related Work

In the last decade, different clustering techniques were proposed to use energy efficiently in wireless resource-constrained nodes. Most of the proposed clustering techniques belong to Wireless Sensor Network (WSN) paradigm. Similar to WSN, nodes in IoT/IoMT play an important role in collecting, sending, and receiving a significant amount of data. Here, we briefly summarize the existing clustering strategies most relevant in our context.

Non-uniform Clustering. In one of the earlier work's, Shu et al. [8] explored the network lifespan maximization problem by balancing the energy consumption among CHs. To obtain balanced energy consumption, two mechanisms are proposed, viz. routing-aware optimal cluster planning and the clustering-aware optimal random relay. The first method uses a clustering approach that is developed under the perspective of shortest path inter-cluster routing. The second method is a routing strategy for load-balanced clustered topologies. Recently, Feng et al. [6] proposed a clustering algorithm to improve the network lifespan of IoT. In the proposed clustering algorithm, initially, the authors used a K-means clustering algorithm to partition the network area into clusters. Particularly, the authors used an objective function to form the clusters. After cluster formation, to avoid uneven energy consumption, the authors proposed a weighted evaluation function to adjust the cluster size. More recently, Halder et al. [4] proposed a clustering structure, where CHs are static and selected during deployment process. In this proposed clustering structure, cluster size is determined by solving an optimization problem, where input parameters are node density, packet size etc. Next, the authors proposed a deterministic deployment algorithm to place CHs and MNs at some designated locations. Different from the earlier works, in [11], authors proposed an energy-aware distributed dynamic clustering protocol, where CHs are selected according to on-demand basis. In the proposed protocol, tentative CHs are selected considering delay times. Finally, the authors use fuzzy logic to assess the fitness cost of the tentative CH to become a CH. The fitness cost is derived considering two metrics, viz. node degree and node centrality.

Uniform Clustering. In a different attempt, Alaei and Ordinas [5] proposed a clustering algorithm, where CHs are selected by the sink. In this algorithm, each cluster size is calculated based on the overlapped area between Field of View of sensors. Recently, Schranz and Rinner [12] proposed

a dynamic clustering technique for IoMT. In the initial round of the proposed technique, CH is elected based on the available resources and a visibility parameter. For the subsequent rounds, CHs are selected based on the auction and CH of previous round initiate the auction process. In an interesting work [9], authors proposed an on-demand clustering protocol, where CH is selected based on the residual energy. To reduce communication overhead, the authors used directed diffusion in their proposed protocol.

In context to non-uniform clustering approaches, we have the following observations. (1) Except the works in [9], [11], none of the works consider the on-demand based clustering approach as a solution to maximize the network lifespan. Therefore, we are motivated to devise an on-demand based clustering protocol. (2) In majority of the literature, residual energy is considered as the only parameter to select a CH, thus, overlooking the possible conflict of several nodes with same residual energy. Motivated by this fact, we considered average energy usage in addition to residual energy level while selecting CH.

III. System Model

In this section, we describe the models used in this work. In particular, Section III-A presents the network model. Section III-B discusses the network operation model. We then introduce the energy model in Section III-C. Finally, in Section III-D, we describe the channel model.

A. Network Model

We consider a network area χ of radius D which is covered by a disk sector of angle ϕ (see Fig. 1) [13]. The disk sector is partitioned into i ring sectors or slices, where $i = 1, \ldots, N$. The sink is considered to be located at the vertex, as shown in Fig. 1, and responsible for gathering data from nodes. Nodes are randomly and uniformly deployed across χ with density ρ. We assume a slice based network area, and argue that this slice shape is general enough to estimate many other shapes like rectangle, triangle and square [8], [13].

In this work, we consider deployment of static heterogeneous IoMT nodes. Here, by heterogeneous node, we mean a node that can regulate its communication range. At present, a node with variable communication range (e.g., like Crossbow IRIS, TelosB motes) is commercially available. For example, Keally et al. [14] designed a real-time human traffic detection mechanism using similar heterogeneous nodes as we considered in this work. Further, we consider continuous monitoring applications like wildlife tracking in which each node captures images continuously, however, it generates imagery data packets only when it has sensed an event (e.g., discovering rare animal species). Once an event is detected, the cluster setup phase is triggered and nodes that detect an event only take part. Rest of the nodes remain in active mode for detecting future event(s) and/or forwarding data packets. For the sake of simplicity, in this paper, the cluster setup phase is divided into two sub-phases, namely, CH selection and cluster building. After cluster setup, each MN acquires imagery data from the surrounding environment, generates n bits data packet, and transmits the data packet to its CH at every round [13]. In contrast, the CH aggregates and forwards the data packets received from both its MNs and neighbouring CHs which are far away from the sink. This process repeats till the data packets arrive at the sink from a MN through intermediate CHs. As we divide the area χ into N slices, thus N types of clusters exist in the network. In particular, the clusters located nearest to the sink are placed in the 1st slice (i.e., 1st type), and the ones farthest from the sink are placed in the N-th slice (i.e., N-th type). In this work, we assume that the MNs whose distances from the sink fall in $(r_{i-1}, r_i]$ are organized into clusters of the i-th type, where $1 \leq i \leq N$ and $r_1 < \ldots < r_N = D$.

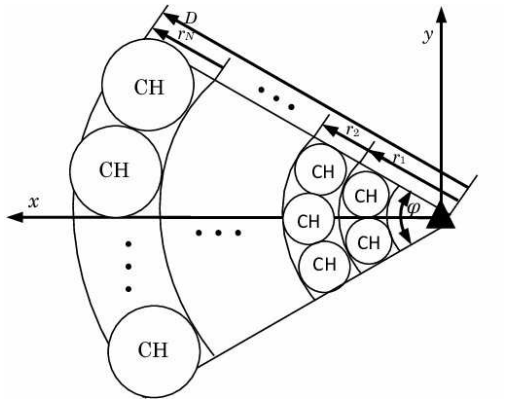

Fig. 1. Network area division into slices.

B. Network Operation

In this work, we assume optimality in both data collection and routing path formation methods as proposed by Lee et al. [15]. In the proposed optimal data collection and routing path formation methods, once the nodes are deployed, network set-up phase starts. In this phase, each node learns about their one-hop neighbours by exchanging messages among themselves and record their assigned node ID. Once the network finishes the set-up phase, the connectivity graph rooted at the sink is formed. Next, to determine the optimal data collection and routing path that balance the overall energy consumption among the nodes, an optimal Directed Acyclic Graph (DAG) is formed based on the connectivity graph. For detailed discussion, the readers may refer to [15]. After the DAG construction, the network is aware about the parent set of node and child set of node. A child node in any slice determines an optimal routing path to forward the data packet to a parent node towards the sink which has the link with the maximum remaining usage and optimal flow for sending its data. Next, the parent node employs the same procedure to choose the next forwardee node for sending its data packet. This process is repeated till the data packet arrives at the sink.

C. Energy Model

In this paper, we consider the most popular energy model, i.e., first order radio model [10], [13], as our energy model,

where wireless transmissions and receptions dominate energy consumption of a node. In addition to transmission and reception, a node (i.e., CH) also consumes energy for data aggregation. According to this model, the energy consumed for transmission and reception is as follows: energy consumption for transmitting an n bits data packet by a node located at i-th slice over an adjustable transmission range R_i is $e^i_{tr}(n, R_i) = (e_{elec} + e_{amp}R_i^2)n = e^i_t n$, where $e^i_t = (e_{elec} + e_{amp}R_i^2)$ and e^i_t is the energy consumed to transmit one bit data by a node located at the i-th slice. In contrast, the energy consumption for receiving and aggregating an n bits data packet is $e_{re}(n) = e_{elec}n = e_r n$, and $e_{da}(n) = e_a n$, respectively, where $e_r = e_{elec}$, e_r and e_a is the energy consumed for receiving and aggregating one bit data, respectively.

Since image compression is also considered as an integral part of IoMT, energy model described above needs slight modifications. According to the experiments on energy consumption in image compression algorithm [16], an image compression enabled node can compress the captured images and reduce the size of packet workload forwarded to the sink. To finish the image compression task, a node has to spend extra processing energy. If k_t is image compression ratio, the energy model considering image compression algorithm in our work can be summarized as: $e^i_{tr}(n, R_i) = k_t e^i_t n$ and $e_{da}(n) = k_{com}e_a n$, where k_{com} is the amplified gain for extra image compression operation and $k_{com} > 1$.

D. Channel Model

In this work, we use a Rician fading model [13] for describing the channel between two CHs, and also between the CH and the sink. In this model, the probability density function of the received signal amplitude is given by:

$$f(\xi) = \frac{\xi}{\sigma^2} e^{-(\xi^2+s^2/2\sigma^2)} I_0\left(\frac{\xi\sqrt{2R_f}}{\sigma}\right),$$

where ξ is a normalized random variable that represents the fluctuation in the fading process, σ^2 is the variance of the multipath components, s is the amplitude of the line-of-sight component, $I_0(\cdot)$ is the zero-order Bessel function of the first kind and R_f is the Rician factor, given by: $R_f = s^2/2\sigma^2$. It is worth noting that as the Rician factor goes to zero, ξ becomes a Rayleigh random variable [17]. In this channel model, for a transmitter-receiver separation distance l, channel gain is given as:

$$h(l) = \frac{G_t G_r \omega^2}{(4\pi l_0)^2}\left(\frac{l}{l_0}\right)^{-\eta}\xi = L(l_0)\left(\frac{l}{l_0}\right)^{-\eta}\xi, \qquad (1)$$

where $L(l_0) = G_t G_r \omega^2/(4\pi l_0)^2$ is the path loss of the close-in distance l_0, G_t and G_r are the corresponding gains of the transmitting and receiving antennas, ω is the wavelength of the carrier signal, η is the path loss exponent ($2 \le \eta \le 6$). Since, ξ is random, correct reception of a signal can be guaranteed only when it is represented on a probabilistic basis. Accordingly, in our work, reliable reception of a signal is represented as $\Pr\{e_{rx} \ge \tau\} \ge \delta_r$, where e_{rx} is the energy of the received signal, τ is a predefined energy threshold and δ_r is the required link reliability.

IV. Analysis on Network Lifespan Maximization

In this section, in contrast to the existing heuristic load balancing based clustering technique, we investigate the clustering technique based on an analytical approach to maximize network lifespan. In our analysis, we consider nodes are arbitrarily placed, however, their locations are known. Further, we consider the definition of network lifespan as:

Network Lifespan. The network lifespan is defined as the time until the first CH dies [8]. A CH is considered as dead when the residual energy is less than a pre-determined threshold, i.e., when it is neither able to transmit nor able to receive any data.

Although the network lifespan from the beginning until the instant at which the last CH dies is measurable using an analytical model, it is not meaningful since the coverage and connectivity cannot be guaranteed in this entire time period. In contrast, the network lifespan from the beginning until the instant at which the network gets partitioned, it totally makes sense. However, time period is not measurable. We thus consider the above definition to make the network lifespan meaningful and measurable. In fact, this definition of network lifespan is application-independent, and thus is suitable for diverse applications.

The average intra-cluster and inter-cluster traffic load carried by the CHs of i-th slice is given by $\pi(r_i^2 - r_{i-1}^2)\rho n\phi/2\pi$ and $\pi(r_N^2 - r_i^2)\rho n\phi/2\pi$, respectively, where $i = 1, \ldots, N$. Note that by network model, the number of CHs in the i-th slice is approximately given by $\frac{2r_i}{r_i - r_{i-1}}\frac{\phi}{2\pi}$. Let E_i^{jk} be the expected energy consumption by CH j in the i-th slice for transmitting all of its traffic to the one-hop neighbor CH k and R_i^{jk} be the distance between these two CHs. It is worth mentioning that the value of E_i^{jk} is different for any two communicating CHs. Therefore, the expected energy consumption by the CH j in the i-th slice is given as:

$$E_i^{jk} = \frac{\pi(r_N^2 - r_{i-1}^2)(r_i - r_{i-1})}{2r_i}\rho n(e_r + e_t^i + e_a), \qquad (2)$$

where $e_t^i = e_{elec} + e_{amp}\left(R_i^{jk}\right)^2$. The expected energy consumption by a CH in the N-th slice can be calculated applying (2) and using the standard convention that a sum of terms is zero if its lower index is greater than its upper bound.

Let e_{ti} be the over-the-air RF energy consumed when transmitting one bit from CH j in the i-th slice to CH k located at distance R_i^{jk}. It is worth mentioning that e_{ti} is a function of the distance between two communicating CHs. So, the above (2) can be rewritten as:

$$E_i^{jk} = \frac{\pi(r_N^2 - r_{i-1}^2)(r_i - r_{i-1})}{2r_i}\rho n(\psi + e_{ti}), \qquad (3)$$

where $\psi = (e_r + e_t^i + e_a)$. From channel model (1), the over-the-air RF energy consumed for receiving one bit, e_{ri}, is given

as:

$$e_{ri} = e_{ti} L(l_0) \left(\frac{R_i^{jk}}{l_0} \right)^{-\eta} \xi.$$

For a Rician fading channel, the link reliability requirement can be expressed as:

$$\delta_r = \Pr\{e_{ri} \geq \tau\} = \Pr\left\{ \xi \geq \frac{\tau}{e_{ti} L(l_0)} \left(\frac{R_i^{jk}}{l_0} \right)^{\eta} \right\}$$
$$= e^{\frac{-\tau}{e_{ti} L(l_0)} \left(\frac{R_i^{jk}}{l_0} \right)^{\eta}}.$$

From the above expression, we can express e_{ti} as:

$$e_{ti} = \frac{-\tau}{L(l_0) \log \delta_r} \left(\frac{R_i^{jk}}{l_0} \right)^{\eta}.$$

According to our routing model (see Section III-B), let h be the maximum number of links of an end-to-end path. Hence, to generate the constraint on path reliability, δ_p, the minimum link reliability must be: $\delta_r = \delta_p^{\frac{1}{h}}$. Therefore,

$$e_{ti} = \frac{-h\tau}{L(l_0) \log \delta_p} \left(\frac{R_i^{jk}}{l_0} \right)^{\eta} = \beta \left(R_i^{jk} \right)^{\eta},$$

where $\beta = -h\tau / L(l_0) l_0^{\eta} \log \delta_p$ and it is a constant. Consequently, the energy consumed by CH j in the i-th slice, given in (3), can be rewritten as:

$$E_i^{jk} = \frac{\pi (r_N^2 - r_{i-1}^2)(r_i - r_{i-1})}{2 r_i} \rho n \left(\psi + \beta \left(R_i^{jk} \right)^{\eta} \right). \quad (4)$$

To maximize the network lifespan, our objective is to compute $\{r_i\}$, where $i = 1, \ldots, N$, for minimizing the maximum energy consumption rate among all the CHs. The calculation procedure can be formulated by the following optimization problem:

$$\max \min \left\{ \frac{e_{in}}{E_1^{jk}}, \ldots, \frac{e_{in}}{E_N^{j'k'}} \right\},$$

where e_{in} is the initial energy of a CH. Introducing an auxiliary variable t, where $t \leq \max \left\{ E_1^{jk}, \ldots, E_N^{j'k'} \right\}$, the above objective function can be transformed into the following optimization problem:

$$\min_{r_1, r_2, \ldots, r_N} t, \quad (5)$$

subject to

$$\frac{\rho n \phi}{2} \left(r_i^2 - r_{i-1}^2 + \sum_{h=i}^{N} \left(r_{h+1}^2 - r_h^2 \right) \right) - \frac{\rho n \phi}{2} \sum_{h=i-1}^{N} \left(r_{h+1}^2 - r_h^2 \right),$$
$$\forall 1 \leq i \leq N \quad (6)$$

$$t \frac{\pi \rho n (r_N^2 - r_{i-1}^2)(r_i - r_{i-1})}{2 r_i} \left(\psi + \beta \left(R_i^{jk} \right)^{\eta} \right) \leq e_{in}, \quad (7)$$

$$\frac{\rho n \phi}{2} \left(r_i^2 - r_{i-1}^2 \right) > 0, \frac{\phi r_i}{2\pi (r_i - r_{i-1})} > 0. \quad (8)$$

The constraint (6) guarantees inter-cluster flow preservation, i.e., all data packets generated at or forwarded to a slice are pushed out of it. The constraint (7) specifies that in the lifespan t no node consumes more than its available energy e_{in}. The constraint (8) specifies that the intra-cluster data flow and number of clusters in a slice is non-negative. If we examine both the objective function and the constraints, the problem is convex. Thus, using interior point method [18], the above problem can be easily solved. To solve (5)-(8), one needs to know network size and network information, e.g., packet size. It is easy to check that the nature of the objective function is convex. It is worth reminding that we consider the nodes in a slice report data to the sink in shortest path, hence the derived lifespan of CH provides the upper bound of the network lifespan.

V. Proposed Clustering Protocol: DISC

In this section, we present the main design of DISC. Particularly, we first describe node deployment strategy in Section V-A. Section V-B presents the cluster setup phase. Finally, in Section V-C, we discuss the data packet collection phase. It is worth mentioning that we already discussed the routing path formation and evaluation of optimal cluster radius in Section III-B and Section IV, respectively.

A. Deployment

In this paper, we consider the stochastic deployment where nodes are dropped in unfriendly environments. In particular, we consider that nodes are uniformly and independently distributed in different slices around the sink. The probability f_a that a point is covered by nodes is:

$$f_a = 1 - e^{-\rho \pi R_s^2}, \quad (9)$$

where R_s is the sensing range a node.

Our objective is to deploy nodes in the slice based network area (see Fig. 1). To achieve this goal, we propose to decompose the i-th slice into multiple circular domains so that each circular domain is regarded as a cluster. Next, the nodes are uniformly and independently distributed within each cluster using (9). After deployment of nodes, without loss of generality, we assume that the IoMT passes thorough a training process where each node learns about the slice and the region to which it belongs. Recently, a number of training protocols were proposed. In this work, we assume a training protocol as proposed in [19].

B. Cluster Setup

In DISC, unlike time driven CH selection, we propose a novel on-demand based CH selection strategy to reduce the extra message overhead during cluster formation. All the nodes in the network are eligible to become CHs, and they are selected through a proposed process. This CH selection process is divided into two sub-phases: CH selection (see Section V-B1) and cluster building (see Section V-B2).

1) CH Selection Sub-phase: The proposed CH selection strategy is triggered once an event of interest (e.g., detection of an intruder) is detected. Node(s) that detects an event (hereafter referred to as detected node) only takes part in the CH selection and cluster building processes. Rest of the nodes remain in active mode for detecting future event(s) and/or forwarding data packets. Upon detecting an event, a detected node poses itself as acting CH and broadcast $Hello(ID, E_i, E_r)$ message around the cluster radius to rest of the detected nodes, where ID, E_i and E_r denote the node identification number, expected energy consumption rate and residual energy level of the detected node, respectively. It is worth mentioning that the cluster radius is determined by solving our optimization problem given in Section IV. However, during inter-cluster communication a CH uses higher energy level so that the transmitted data packet can reach atleast two or more cluster diameters. Henceforth, for the sake of simplicity, we call "rest of the detected nodes within cluster radius" as neighbours of the acting CH. After a detected node receives the $Hello$ message, all the neighbours send $Hello\_Ack(ID, E_i, E_r)$ message to the acting CH. The acting CH calculates average energy consumption (AE_i) and average residual energy (AE_r) based on the number of $Hello\_Ack(ID, E_i, E_r)$ messages, N_e, received from the neighbouring nodes. The acting CH nominates the k-th node from the neighbours within the cluster radius as new CH whose E_i is minimum, i.e., $AE_i > \ldots > E_i^{min}$, and E_r is maximum, i.e., $AE_r < \ldots < E_r^{max}$. If there is more than one node with the same $\left(E_i^{min}, E_r^{max}\right)$, one of them is chosen randomly. We calculate AE_i and AE_r as follows:

$$AE_i = \sum_i^N \frac{E_i}{N_e}, AE_r = \sum_i^N \frac{E_r}{N_e}.$$

2) Cluster Building Sub-phase: After CH selection, the newly selected CH broadcasts a selection message, $Head\_Msg$, within the cluster radius by regulating communication range R_i. The $Head\_Msg$ message contains node ID, present energy consumption rate and residual energy. After receiving $Head\_Msg$ message, a node responds to the newly selected CH by sending $Join\_Msg$ message. If a node receives more than one $Head\_Msg$ message from its neighbouring CH, it will choose to join the nearest CH by sending $Join\_Msg$ message. Here, we assume that a node calculates the distances between itself and neighbouirng CHs based on received signal strength. Detailed discussion of distance calculation based on received signal strength is out of the scope of this work. For detailed discussion, the readers may refer to [20]. The CH on receiving $Join\_Msg$ message acknowledges the joined node by sending $Head\_Acpt$ message and designate that joined node as MN. As a CH can regulate its communication range, thus no node in the network is left away from the cluster framework.

C. Data Packet Collection

After the cluster formation, each CH in the network generates a Time Division Multiple Access (TDMA) schedule for its MNs. In TDMA, the available bandwidth is normally divided into frames and each frame is divided into time slots. The length of the frame depends on the number of MNs and time allotted for each MN for data transmission. In this work, we assumed that all the MNs are assigned the same amount of time slots and the length of the frame is decided based on the number of received $Join\_Msg$ messages. After receiving the schedule, each MN sends its sensed data to its CH by following the TDMA schedule. MNs are awake only during their allotted time slot(s) for transmission and sleep for rest of the time. However, a CH remains in an active/awake state to receive sensory data from its MNs. Since the data gathered by the CHs are highly correlated, hence each CH aggregates the received data packets into a single data packet. Finally, at the end of the frame, the aggregated data packets are sent to the sink through intermediate CHs. In case, if there is no CH, then intermediate nodes from the optimal DAG (see Section III-B) are chosen to forward the data packets. A typical time line of operation of our proposed algorithm is illustrated in Fig. 2.

In IoMT, due to the broadcast nature of wireless links, when a MN transmits a packet to its CH, in some cases, the packet may reach to the nearby CHs. To avoid this inter-cluster interference, we assumed that the MN uses spread code. Particularly, when the MNs send the packet to their respective CHs, the spread code of the concerned cluster is attached to avoid inter-cluster interference.

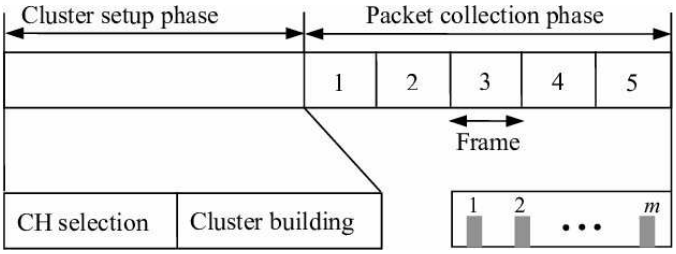

Fig. 2. Time line of DISC.

VI. Experimental Evaluation

In this section, we compare the performance of DISC with that of two recent clustering algorithms, namely, Delay-constraint Unequal Clustering based on weighted Function (DUCF) [6] (belong to IoT domain), and Energy Level based Passive Clustering (ELPC) [9] (belong to IoMT domain). To make the performance comparison more realistic, we consider two variants of DISC, DUCF and ELPC. In one variant, we consider channel model as Rician fading whereas, in another variant Rayleigh fading is considered. Since IoMT can operate in both indoor and outdoor environments, we consider these two popular channel models while measuring the performance of all the competing schemes. It is worth noting that Rician fading is particularly suitable for indoor environment, whereas, Rayleigh fading is particularly suitable for outdoor environment [17]. During implementation of DUCF and ELPC, similar to DISC, we considered that nodes are randomly and uniformly deployed in the network area.

A. Experimental Setup

For performing the experiments, we used MATLAB simulator. During experiment, we use a real-world publicly-available dataset for pedestrian detection [21]. In our experiments, we deployed nodes in an area consisting of 6 slices at an angle $\phi = 60^0$. During experiment, nodes are distributed in such a way that nodes with smaller ID numbers are closer to the sink, whereas, those with larger ID numbers are far away from the sink. We simulate all the schemes under both ideal and realistic scenarios. In ideal scenario, the nodes used routing protocol as stated in Section III-B, MAC layer as ideal, and consume energy for transmission, reception, sensing and processing. On the contrary, in realistic scenario, the nodes additionally use a MAC layer protocol which includes idle/sleep schedule. Moreover, unlike the ideal scenario, in realistic scenario, energy consumption is considered for sensing, remaining idle, and sleeping in addition to transmission, reception and aggregating. Further, energy consumption rates for sensing, remaining idle, and sleeping are considered as 20%, 5%, and 2.5% of the energy consumption rate of reception [22], respectively. The communication between CHs considers Receiver-Centric Medium Access Control (RC-MAC) protocol [23] as the underlying MAC protocol. RC-MAC protocol is specially designed for on-demand application scenario. Finally, we considered a video sequence with the spatial resolution of 1280×720 pixels, and the frame rate as 60 frames per second. The video sequence is encoded using a fast implementation of H.264/AVC [22] at various quantization step sizes, with a group of pictures length of 25 and a frame rate of 60 frames per second.

The width of a slice in the network is obtained by solving (5)-(8) using CVX solver [24]. To make the comparison fair, we deployed 200 nodes, and a sink is deployed at the coordinate (0, 0). In simulation experiment, for all the schemes, we consider that once an event of interest is captured by a node, it generates packets at the constant bit rate of 40 kbps and transmits over bandwidth 1 Mbps, whereas duration of each data gathering round is 20 sec. Unless specified otherwise, we use the following parameters throughout the experiment: $R_f = 20$, $R_s = 10$ m, $e_t = 60$ nJ, $e_r = e_a = 50$ nJ, $e_{in} = 50$ J, $n = 400$ bits, $k_{com} = 1.2$, $k_t = 55\%$, $l_0 = 10$ m, $G_t = G_r = 1$, $\tau = 10^{-17}$, $\eta = 4$, $\delta_r = 0.99$ and $\omega = 0.125$ m (2.40 GHz). We consider the energy cost to run the transmitter/receiver radio circuitry per bit processed as (e_{elec}) 50 nJ/bit. Also, we consider the energy used by the transmitter amplifier (e_{amp}) to achieve an acceptable signal to noise ratio (30 dB) as 10 pJ/bit/m^2. Furthermore, we use the same parameters with same values for RC-MAC protocol as described in [23]. Extensive simulation is performed with a 95% confidence level and average results of 200 independent runs are taken while plotting the results.

B. Performance Metrics

To evaluate the performance of DISC, DUCF and ELPC, we conducted three sets of experiments, where, first set measures energy balancing in the network, second set verifies the enhancement of network lifespan, and final set measures the Peak Signal-to-Noise Ratio (PSNR). In our experiment, energy balance is measured using Average Energy Consumption Rate per CH (Avg ECR per CH) in a slice as given in (5). We consider network lifespan as defined in Section IV, and PSNR is measured as: the mean square error of each pixel between the original and received images [22]. For the sake of clarity, in simulation plots, schemes named with '(R)' signify performances in realistic scenario and the schemes with '(I)' denote performances in ideal scenario.

C. Energy Balance

Figure 3 shows avg ECR per CH for both indoor and outdoor environments. Here, we observe that in DISC, irrespective of scenarios, the plots of avg ECR per CH for both the environments are fairly constant for all slices. For example, in indoor environment, avg ECR per CH is 12.51 μJ/sec and 21.83 μJ/sec for ideal and realistic scenarios, respectively. In contrast, in outdoor environment, it is 25.70 μJ/sec and 45.36 μJ/sec for ideal and realistic scenarios, respectively. It is worth noting that, in DISC, avg ECR per CH is significantly less compared to all the competing schemes irrespective of scenario and environment. Particularly, the plot shows that DISC outperforms the other schemes. Further, it is noticed that, among all the schemes, avg ECR per CH is highest in DUCF and lowest in DISC. For example, avg ECR per CH of DISC is 108% and 45% less than that of DUCF and ELPC, respectively during ideal scenario in indoor environment. Similarly, DISC is 46.15% and 25.15% less than that of DUCF and ELPC, respectively during ideal scenario in outdoor environment. This is due to the fact that, in DISC, the CH selection process is optimal and energy efficient compared to DUCF and ELPC. Further, irrespective of environment, CHs in 1st slice of both DUCF and ELPC have maximum avg ECR per CH, whereas, CHs in the farthest slice have lowest avg ECR per CH. Interestingly, irrespective of scenario and environment, avg ECR per CH plots of DISC are relatively steady throughout the slices. This indicates that DISC is more energy balanced compared to DUCF and ELPC. Similar to the ideal scenario, in the realistic scenario, the plot of avg ECR per CH for all the competing schemes are more or less the same. For all the schemes, if we compare the results of both the scenarios (irrespective of environment), it is observed that in all the cases avg ECR per CH in realistic scenario is higher compared to avg ECR per CH in ideal scenario. The additional energy usage for realistic scenario is due to the implementation of MAC protocol. Finally, it is noticed that avg ECR per CH is higher in outdoor environment compared with indoor environment. It is expected, since the propagation condition is more severe in outdoor environment, causing more number of re-transmissions, eventually resulting in higher avg ECR per CH.

D. Network Lifespan

Figure 4 shows the network lifespan of all the competing schemes in indoor and outdoor environments. It is observed

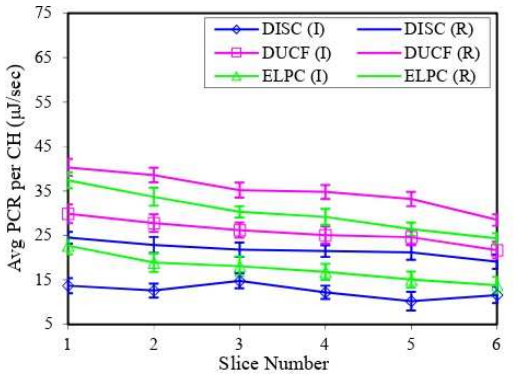

(a) Indoor environment

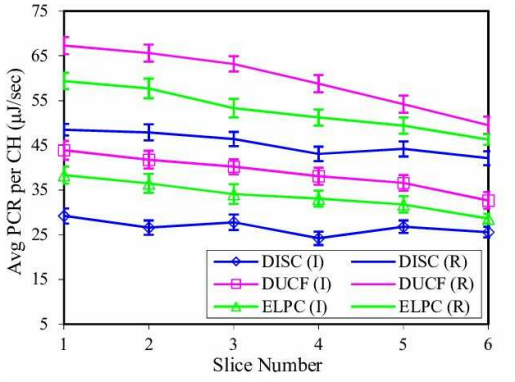

(b) Outdoor environment

Fig. 3. Average energy consumption rate per CH in ideal and realistic scenarios.

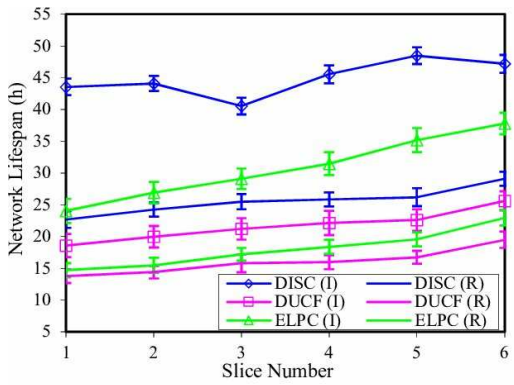

(a) Indoor environment

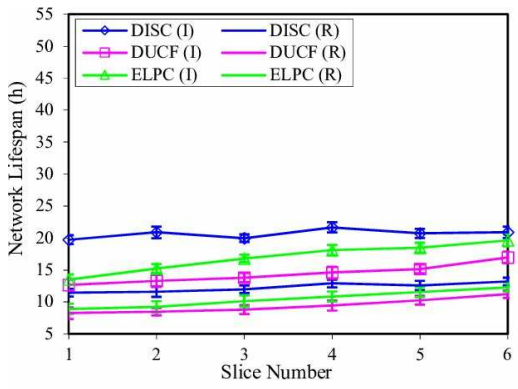

(b) Outdoor environment

Fig. 4. Network lifespan in ideal and realistic scenarios.

from the plot that DISC outperforms the other schemes. In particular, for indoor environment, it is observed from Fig. 4(a) that the network lifespan of DISC is 93.17% and 32.25% more than that of DUCF and ELPC, respectively, during ideal scenario, whereas, in realistic scenario, it is 59.67% and 37.42% more than that of DUCF and ELPC, respectively. Similar to Fig. 4(a), the nature of plot for different competing schemes follow similar characteristic in Fig. 4(b). Moreover, in DISC, nearly flat nature of the plot ensures that in all the slices, network lifespan terminates in more or less the same time as compared to DUCF and ELPC. This ensures that energy in DISC is balanced to a greater extent than both the competent schemes.

Summarily, for all the schemes, if we compare the experimental results of network lifespan under both scenarios and environments, it is reduced in realistic scenario, as there is additional energy consumption due to implementation of MAC protocol. Finally, irrespective of scenario, if we compare the performance of all the schemes under indoor and outdoor environments, network lifespan is lowest in outdoor environment. This is because of harsh propagation conditions in outdoor environment, eventually resulting in lowest network lifespan.

E. PSNR

In this section, we examine the performance of all the strategies in terms of the received video quality measured through the value of the PSNR. During conducting of the experiment, we consider realistic scenario. Fig. 5 shows the PSNR of all the competing schemes in both indoor and outdoor environments. We observe from Fig. 5 that the proposed DISC protocol performs well in both environments. In particular, DISC significantly outperforms DUFC and ELPC. For example, in indoor environment (refer Fig. 5(a)), the average PSNR value of DISC is 14.28% and 26.04% more than that of DUCF and ELPC, respectively. On the contrary, in outdoor environment (refer Fig. 5(b)), the average PSNR value of DISC is 12.26% and 24.17% more than that of DUCF and ELPC, respectively. For all the schemes, if we compare the results of both indoor and outdoor environments, it is observed that the average PSNR is more in indoor environment compared to outdoor environment. It is due to the fact that the propagation condition is more severe in outdoor environment, causing degradation of the video quality received at the sink and thus the poor PSNR.

VII. Conclusion

In this work, we analyzed the problem of network lifespan maximization by balancing energy consumption at different CHs in IoMT. Analysis revealed the optimal cluster radius of each level have significant role in maximization of network lifespan by avoiding energy hole [22]. Considering the results of this analysis, we developed DISC, an on-demand,

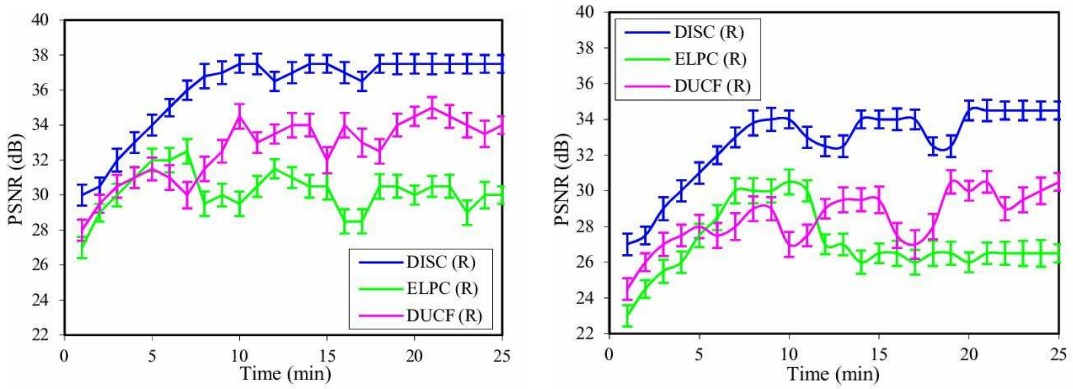

(a) Indoor environment (b) Outdoor environment

Fig. 5. Performance comparison in terms of PSNR.

distributed optimal clustering protocol where CHs are selected dynamically for efficient energy usage among the nodes. The use of on-demand based clustering mechanism reduces clustering overhead because no clusters are maintained unless they are needed. Extensive simulations are performed to measure the performance of the proposed DISC protocol. Simulation results clearly demonstrate that our proposed protocol achieves more than 32% network lifespan compared to two state-of-of-the-art non-uniform clustering protocols [6], [9]. As future work, we seek to study the proposed clustering strategy by including more realistic scenario, such as mobility of CH.

ACKNOWLEDGMENT

This work was supported by the European Commission under the Horizon 2020 Programme (H2020), as part of the LOCARD project (Grant Agreement no. 832735).

REFERENCES

[1] A. Al-Fuqaha, M. Guizani, M. Mohammadi, M. Aledhari, and M. Ayyash, "Internet of things: A survey on enabling technologies, protocols, and applications," *IEEE Communications Surveys & Tutorials*, vol. 17, no. 4, pp. 2347–2376, 2015.

[2] S. A. Alvi, B. Afzal, G. A. Shah, L. Atzori, and W. Mahmood, "Internet of multimedia things: Vision and challenges," *Ad Hoc Networks*, vol. 33, pp. 87–111, 2015.

[3] L. Xu, R. Collier, and G. M. O'Hare, "A survey of clustering techniques in wsns and consideration of the challenges of applying such to 5G IoT scenarios," *IEEE Internet of Things Journal*, vol. 4, no. 5, pp. 1229–1249, 2017.

[4] S. Halder, A. Ghosal, and M. Conti, "LiMCA: an optimal clustering algorithm for lifetime maximization of internet of things," *Wireless Networks*, pp. 1–19, DOI:10.1007/s11276-018-1741-0, 2018.

[5] M. Alaei and J. M. Barcelo-Ordinas, "Node clustering based on overlapping fovs for wireless multimedia sensor networks," in *Proc. of IEEE Wireless Communication and Networking Conference (WCNC)*, 2010, pp. 1–6.

[6] X. Feng, J. Zhang, C. Ren, and T. Guan, "An unequal clustering algorithm concerned with time-delay for internet of things," *IEEE Access*, vol. 6, pp. 33 895–33 909, 2018.

[7] P. Neamatollahi, M. Naghibzadeh, S. Abrishami, and M. H. Yaghmaee, "Distributed clustering-task scheduling for wireless sensor networks using dynamic hyper round policy," *IEEE Transactions on Mobile Computing*, vol. 17, no. 2, pp. 334–347, 2018.

[8] T. Shu and M. Krunz, "Coverage-time optimization for clustered wireless sensor networks: a power-balancing approach," *IEEE/ACM Transactions on Networking*, vol. 18, pp. 202–21, 2010.

[9] H. Zeghilet, M. Maimour, N. Badache, and F. Lepage, "On the use of passive clustering in wireless video sensor networks," *International Journal of Sensor Networks*, vol. 11, no. 2, pp. 67–80, 2012.

[10] H. Lin and H. Uster, "Exact and heuristic algorithms for data-gathering cluster-based wireless sensor network design problem," *IEEE/ACM Transactions on Networking*, vol. 22, no. 3, pp. 903–916, 2014.

[11] H. Taheri, P. Neamatollahi, O. M. Younis, S. Naghibzadeh, and M. H. Yaghmaee, "An energy-aware distributed clustering protocol in wireless sensor networks using fuzzy logic," *Ad Hoc Networks*, vol. 1o, no. 7, pp. 1469–1481, 2012.

[12] M. Schranz and B. Rinner, "Resource-aware dynamic clustering utilizing state estimation in visual sensor networks," *Sensors & Transducers*, vol. 191, no. 8, pp. 28–39, 2015.

[13] S. Halder and A. Ghosal, "A predetermined deployment technique for lifetime optimization in clustered wsns," in *Proc. of 15th International Conference on Algorithms and Architectures for Parallel Processing (ICA3PP)*. LNCS-9531, 2015, pp. 682–696.

[14] M. Keally, G. Zhou, G. Xing, D. T. Nguyen, and X. Qi, "A learning-based approach to confident event detection in heterogeneous sensor networks," *ACM Transactions on Sensor Networks*, vol. 11, pp. 1–28, 2014.

[15] H. Lee, A. Keshavarzian, and H. Aghajan, "Near-lifetime-optimal data collection in wireless sensor networks via spatio-temporal load balancing," *ACM Transactions on Sensor Networks*, vol. 6, no. 3, p. 26, 2010.

[16] L. Ferrigno, S. Marano, V. Paciello, and A. Pietrosanto, "Balancing computational and transmission power consumption in wireless image sensor networks," in *Proc. of IEEE Symposium on Virtual Environments, Human-Computer Interfaces and Measurement Systems*, 2005, pp. 61–66.

[17] G. S. Prabhu and P. M. Shankar, "Simulation of flat fading using matlab for classroom instruction," *IEEE Transactions on Education*, vol. 45, no. 1, pp. 19–25, 2002.

[18] D. G. Luenberger and Y. Ye, *Linear and Nonlinear Programming*. USA: Springer Science and Business Media, 2008, vol. 116.

[19] F. Barsi, A. A. Bertossi, C. Lavault, A. Navarra, S. Olariu, M. C. Pinotti, and V. Ravelomanana, "Efficient location training protocols for heterogeneous sensor and actor networks," *IEEE Transactions on Mobile Computing*, vol. 10, no. 3, pp. 377–391, 2011.

[20] S. Tomic, M. Beko, and R. Dinis, "3-d target localization in wireless sensor networks using rss and aoa measurements," *IEEE Transactions on Vehicular Technology*, vol. 66, no. 4, pp. 3197–3210, 2017.

[21] S. Zhang, R. Benenson, and B. Schiele, "Citypersons: A diverse dataset for pedestrian detection," *Proc. of IEEE Conference on Computer Vision and Pattern Recognition (CVPR)*, vol. 1, no. 2, pp. 3213–3221, 2017.

[22] S. Halder and A. Ghosal, "A location-wise predetermined deployment for optimizing lifetime in visual sensor networks," *IEEE Transactions on Circuits and Systems for Video Technology*, vol. 26, no. 6, pp. 1131–1145, 2016.

[23] P. Huang, C. Wang, and L. Xiao, "RC-MAC: a receiver-centric mac protocol for event-driven wireless sensor networks," *IEEE Transactions on Computers*, vol. 64, no. 4, pp. 1149–1161, 2015.

[24] M. Grant and S. Boyd, "CVX: matlab software for disciplined convex programming, version 2.0 beta," [Online]: http://cvxr.com/cvx, Accessed on April 18, 2018.